© 2010 The Chemical Society of Japan Bull. Chem. Soc. Jpn. Vol. 83, No. 8, 887–891 (2010) 

# Quasiclassical Trajectory Calculations of the Isotope Effect: Chemical Stereodynamics for the H(D) + FCl ($v = 0$–3, $j = 0$–3) → HCl(DCl) + F Reactions

**Yanrong Peng**

College of Environmental Science and Engineering, Hunan University, Changsha 410082, P. R. China

Key Laboratory of Environmental Biology and Pollution Control (Hunan University), Ministry of Education, Changsha 410082, P. R. China

Received January 26, 2010; E-mail: pengyr@hotmail.com

A comparative quasiclassical trajectory study of the H + FCl ($v = 0$–3, $j = 0$–3) → HCl + F reaction and its isotope variant has been carried out to investigate the isotope effect from a chemical stereodynamics view point. Employing the recent DHTSN PES of the ground $1^2A'$ electronic state [Deskevich et al., *J. Chem. Phys.* **2006**, *124*, 224303], the present study calculated the angular distributions and the four polarization-dependent differential cross sections characterizing the vector correlations among the product angular momentum $\boldsymbol{j}'$ and the reagent and the product initial relative velocities $\boldsymbol{k}$ and $\boldsymbol{k}'$. The investigated collision energies are 20 and 40 kcal mol$^{-1}$. The study revealed stronger product polarization behaviors in the heavier isotope variant which can be explained with the proposed impulse model for triatomic collision systems.

Isotope effects play an important role in the investigation of reaction dynamics. The remarkable mass ratio, i.e., a mass factor of 2 between deuterium D and protium H, leads to the differences in rate constant of chemical reaction, that is, the kinetic isotope effects (KIEs). Large primary KIEs, due to isotope substitution at the site of bond-forming or bond-breaking, usually indicate a dominant hydrogen-abstraction reaction mechanism, while secondary KIEs, due to isotope substitution at the site of spectator, usually provide information for the transition state (TS) of a chemical reaction. Large secondary KIEs indicate product-like TS while small secondary KIEs reactant-like TS. Hence, it is well known that isotope effects can serve as a sensitive probe to explore interesting issues in chemical reactions.

From a chemical stereodynamics view point, the present work investigates the isotope effect in the FHCl system, which is of special interest in these attractive issues in elementary chemical reaction, such as reactive resonance,[1–3] nonadiabatic processes,[4–8] and mass combination.[9,10] As far as we know, dynamic data, in particular stereodynamical data for the title reactions are very sparse.[11] But their reverse reactions, HCl(DCl) + F → HF(DF) + Cl, have been investigated in detail by several groups both experimentally and theoretically. Rovibrational distribution of the product HF($v', j'$) has been measured at 300 and 1700 K by Ding et al.,[12] with the most populated product states being observed to be $v' = 2, j' = 8$–12. The temperature-dependent rate constant in a temperature range of 195–373 K has been measured by Würzberg and Houston[13] and by Moore et al.,[14] revealing strongly non-Arrhenius behavior. The recent crossed molecular beam experiments of Zolot and Nesbitt[15] measured the product rovibrational distribution at the collision energy of 4.3 kcal mol$^{-1}$ (1 kcal mol$^{-1}$ = 4.184 kJ mol$^{-1}$), reporting highly inverted vibrational distributions with populations of 14%, 34%, 44%, and 8% for $v' = 0$–3 of the product HF. On the other hand, based on several versions of the potential energy surface of the FHCl system,[11,16–18] both quantum dynamics and quasiclassical trajectory (QCT) calculations[19–22] have been performed for the HCl + F → HF + Cl reaction and its isotope variant to explore the relevant issues such as the effect of rotational and vibrational excitations of the HCl(DCl) molecule, tunneling, and Coriolis coupling effects.

Of the different versions of the PES available now for performing dynamics study, the DHTSN PES[18] of the ground $1^2A'$ electronic state is the most recent, constructed at high computational level. The DHTSN PES has a bend FHCl transition state, with a FHCl bending angle of 123.5° and a bond length (HF, HCl) of 2.69$a_0$ and 2.52$a_0$. The DHTSN PES has been previously employed in a number of recent dynamics calculations[20–22] and has proven to be the most accurate. Due to that, the present study also employed this accurate DHTSN PES. The QCT procedure employed here was developed by Han and co-workers.[23,24] In their pioneering earlier work on F/Na + $CH_3I$ reactions,[25] they first applied the QCT method to chemical stereodynamics, calculating the product rotational alignment parameters for these reactions. Later, they improved their developed QCT procedure with an incorporation of a very efficient sympletic integrator into the integration scheme.[26] Fruitful recent studies published in the literature have employed this computational code. There are also many other well-developed quantum and QCT methods that can be used to treat the stereodynamic features of a chemical reaction, to name a few, those of Aoiz and co-workers,[27,28] Aquilanti and co-workers,[29,30] and Balint-Kurti and co-workers.[31,32]

Published on the web July 15, 2010; doi:10.1246/bcsj.20100022

The isotope effect on chemical stereodynamics is investigated at the following two collision energies of 20 and 40 kcal mol$^{-1}$, with emphasis on mass influences on the following computed stereodynamic quantities from the present QCT procedure: the two angular distributions [$P(\theta_r)$ and $P(\phi_r)$] and the four polarization-dependent differential cross sections (PDDCSs). These two collision energies are chosen because they are large enough to ensure the easy occurrence of the chemical process in the title reactions and thus perhaps will be easily realized experimentally. The remainder of the article is organized as follows: the second section introduces the DHTSN PES and the basic lines of this QCT procedure to generate the above-mentioned dynamic quantities, followed by the computed results and discussion in the third section. The last summarizes the article.

## Theory for Chemical Stereodynamics

**The DHTSN PES.** As described in Ref. 18, the analytical functional form of the DHTSN PES employed in the present stereodynamical calculation was fitted to the ab initio energy points. In order to characterize the nonadiabatic features of the FHCl system, ab initio calculations with MOLPRO in the work[18] were carried out using the dynamically weighed multiconfigurational self-consistent field (DW-MCSCF) with internally contracted multireference configuration interaction (MRCI) and the multireference Davidson correction MRCI+Q. The internally contracted MRCI calculation employed orbitals from DW-MCSCF calculation as reference states, using a full valence complete active space including 15 active orbitals (12A′, 3A″). Further, extrapolation to the complete basis set (CBS) limit using the standard aug-cc-PVnZ ($n = 2$, 3, and 4) basis sets of Dunning and co-workers,[33] and external correlation energy scaling were implemented to refine the DHTSN PES.[18] As a consequence, the DHTSN PES is the most accurate thus far, reproducing satisfactory properties of the FHCl system as compared with experimental measurements. For example, the experimental exothermicity of $-33.06$ kcal mol$^{-1}$ of F + HCl → HF + Cl has well been reproduced, nonadiabatic features are also well described by the PES with strongly bent F–H–Cl transition state geometry and two conical intersection seams accessible at low collision energies. Interested readers please refer to Ref. 18 for other important features of this PES.

**Stereodynamical Quantities.** Figure 1 is the center of mass (CM) frame which is used to depict the relationship between the three considered vectors: the reagent and product initial relative velocity vectors $\boldsymbol{k}$ and $\boldsymbol{k}'$, the product angular momentum vector $\boldsymbol{j}'$. As shown in the CM frame, the $z$ axis is parallel to $\boldsymbol{k}$, the $zx$ plane contains $\boldsymbol{k}$ and $\boldsymbol{k}'$ and is therefore called the scattering plane, and the $y$ axis is perpendicular to this scattering plane. $\theta_r$ defines the angle between $\boldsymbol{j}'$ and $\boldsymbol{k}$, $\Phi_r$ defines the dihedral angle of the two planes containing $\boldsymbol{k}'$ and $\boldsymbol{k}$, $\boldsymbol{k}$ and $\boldsymbol{j}'$ respectively. The polar angles of $\theta_r$ and $\Phi_r$ together define the direction of $\boldsymbol{j}'$. $\theta_t$ defines the scattering angle between $\boldsymbol{k}$ and $\boldsymbol{k}'$ in the scattering plane. All these angles can be calculated in the QCT procedure where the Hamiltonian of motion is solved by a six-order symplectic integrator,[26] then are further used in the following expansion formulae[23,24] to obtain the stereodynamic quantities which can provide information on vector correlations $\boldsymbol{j}'$–$\boldsymbol{k}$ and $\boldsymbol{k}'$–$\boldsymbol{k}$–$\boldsymbol{j}'$:

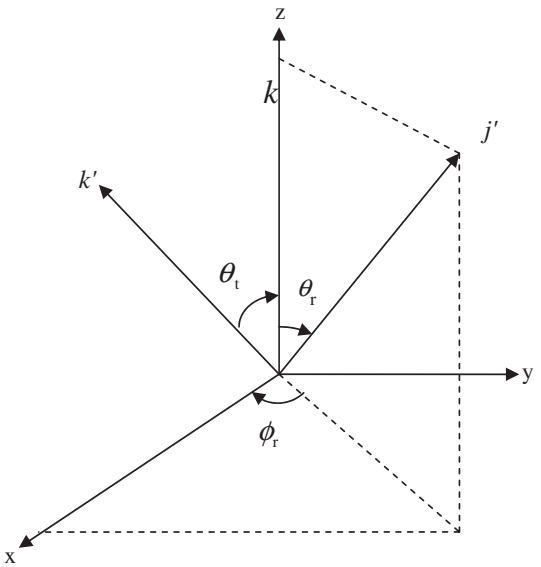


**Figure 1.** The center of mass frame used in the present QCT calculation.

$$P(\theta_r) = \frac{1}{2}\sum_k [k] a_0^k P_k(\cos\theta_r),\ [k] = 2k+1,\ a_0^k = \langle P_k(\cos\theta_r)\rangle \tag{1}$$

$$P(\phi_r) = \frac{1}{2\pi}\left(1 + \sum_{n(even\geq 2)} a_n \cos n\phi_r + \sum_{n(odd\geq 1)} b_n \sin n\phi_r\right)$$
$$a_n = 2\langle \cos n\phi_r\rangle,\quad b_n = 2\langle \sin n\phi_r\rangle \tag{2}$$

$$\frac{1}{\sigma}\frac{d\sigma_{kq\pm}}{d\omega_t} = \sum_{k_1}\frac{[k_1]}{4\pi} S_{kq\pm}^{k_1} C_{k_1 q}(\theta_t, 0)$$
$$S_{kq\pm}^{k_1} = \langle C_{k_1 q}(\theta_t, 0) C_{kq}(\theta_r, 0)[(-1)^q e^{iq\phi_r} \pm e^{-iq\phi_r}]\rangle \tag{3}$$

where the angular bracket represents an average over all reactive trajectories (or and over all angles) and $C_{kq}$ represents the modified spherical harmonics. $\frac{1}{\sigma}\frac{d\sigma_{kq\pm}}{d\omega_t}$ is called the PDDCSs. Usually, the procedure generated four PDDCSs with $kq\pm = 00$, 20, 21−, 22+. These four PDDCSs are chosen to be computed and analyzed because they are measurable quantities, for which there exists a possibility of making a future comparison between theory and experiment. The truncated number in the expansions is: $k = 18$, $n = 24$, $k = 7$, and $k_1 = 7$. Consequently, vector correlation of product angular momentum $\boldsymbol{j}'$ with $\boldsymbol{k}$ can be directly provided by $P(\theta_r)$, vector correlation of $\boldsymbol{j}'$ with $\boldsymbol{k}$–$\boldsymbol{k}'$ can be directly provided by $P(\phi_r)$. Information on scattered product can be directly read from $PDDCS_{00}$ which is the usual differential cross section. Although somewhat indirectly, information on product alignment can also be provided by $PDDCS_{20,21-,22}$ by comparing with their limited values.

In the present QCT calculation, the initial orientation of the reagent angular momentum $\boldsymbol{j}$ is randomly sampled. The initial distance between the attacking atom H(D) and the center of mass of the diatomic molecule FCl is set to 10 Å. An integration step of 0.1 fs is sufficient for getting convergent results. 50000 trajectories are run on the ground potential energy surface of the FHCl system for the two collision energies of 20 and 40 kcal mol$^{-1}$. For H(D) + FCl ($v = 0$,

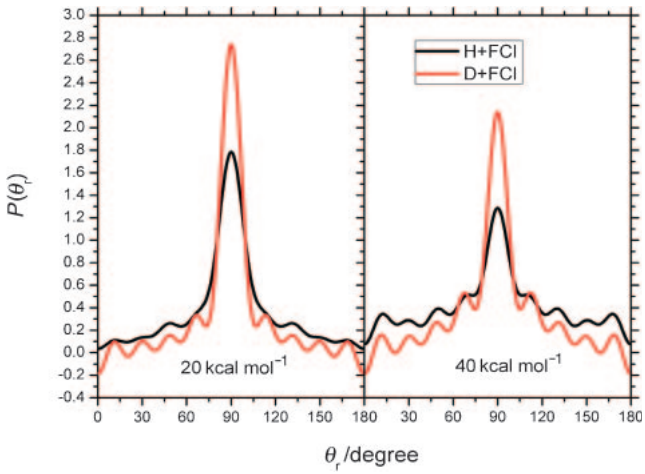


**Figure 2.** Comparison of the $P(\theta_r)$ distributions between the H + FCl ($v = 0, j = 0$) → HCl + F and the D + FCl ($v = 0, j = 0$) → DCl + F reactions for the two collision energies of 20 and 40 kcal mol$^{-1}$.

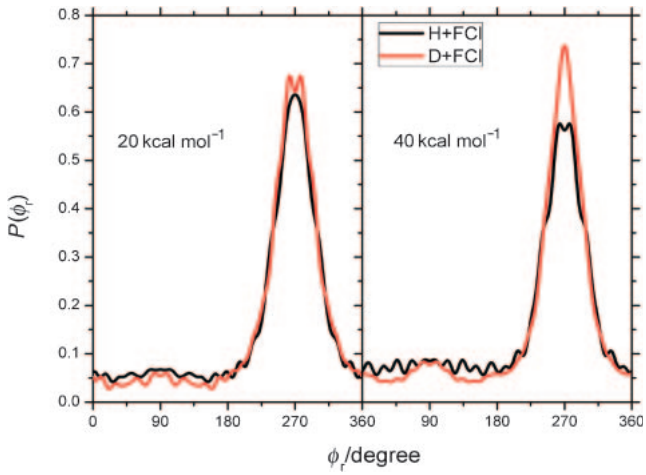


**Figure 3.** Comparison of the $P(\phi_r)$ distributions between the H + FCl ($v = 0, j = 0$) → HCl + F and the D + FCl ($v = 0, j = 0$) → DCl + F reactions for the two collision energies of 20 and 40 kcal mol$^{-1}$.

$j = 0$), the optimized maximum impact parameters at the two collision energies are 2.25 (2.45) and 2.32 (2.4) Å, respectively. For $v = 1$–3 in H(D) + FCl ($v, j = 0$) at the collision energy 20 kcal mol$^{-1}$, these values are 2.46(2.6), 2.63(2.75), and 2.66(2.85) Å, respectively. While for $j = 1$–3 in H(D) + FCl ($v = 0, j$) at the same collision energy, they changed to 2.28(2.43), 2.3(2.43), and 2.28(2.43) Å.

## Results and Discussion

Figure 2 compares the $P(\theta_r)$ distributions at the two collision energies of 20 and 40 kcal mol$^{-1}$ between the D + FCl ($v = 0$, $j = 0$) and the H + FCl ($v = 0, j = 0$) reactions. With an obvious peak located at $\theta_r = 90°$, the calculated distribution indicates that both reactions show a preference for perpendicular alignment to $\boldsymbol{k}$ of the product angular momentum, and such product alignment perpendicular to $\boldsymbol{k}$ is found to be much stronger in the isotope variant. Therefore, isotope substitution exerts substantial influence on product alignment indicated by $P(\theta_r)$. Further, the two reactions show similar trend where product alignment becomes weaker with increasing collision energy, thus it seems that isotope substitution do not changes the energy-dependent behavior of this kind of product alignment.

Figure 3 presents the calculated $P(\phi_r)$ distributions for the two reactions at the two investigated collision energies. As seen, influence of the isotope substitution lies in that the H + FCl reaction illustrates somewhat weaker product polarization behaviors. That is, both the product alignment perpendicular to the scattering plane (evidenced by the two peaks at $\phi_r = 90°$ and $\phi_r = 270°$) and the product orientation pointing to the negative direction of the $y$ axis (evidenced by the remarkable larger peak at $\phi_r = 270°$) are rather stronger in isotope variant. Different from the decreasing trend of the $\phi_r = 270°$ peak height with increasing collision energy observed in H + FCl, there is an increasing trend in D + FCl, which eventually leads to the growing difference in $P(\phi_r)$ distributions, in particularly with the $\phi_r = 270°$ peak, between the two reactions at high collision energy. Therefore, we can say that isotope substitution influences not only the product polarization behaviors described by the $P(\phi_r)$ distribution but also their energy-dependent behaviors.

It was found that the energy redistribution among the product vibrational and rotational modes changes when increasing collision energy from 20 to 40 kcal mol$^{-1}$. For both reactions and at higher collision energy, there is much more energy redistributed into product rotational mode than vibrational mode. It is surmised that product alignment perpendicular to $\boldsymbol{k}$ indicated by $P(\theta_r)$, is possibly hampered by this increasing trend in product average rotational energy with increasing collision energy, thus leading to the similar energy-dependent behaviors of $P(\theta_r)$ for both reactions. Based on the impulse model[34] which will be given in detail in the later part of this article, the asymmetric $P(\phi_r)$ distribution is mainly correlated with the impulsive energy and with $m_{HCl}(m_{DCl})$. Therefore, it is very likely that a combined interaction of these two factors is responsible for the opposite trend of the two reactions concerning the energy-dependent behaviors of $P(\phi_r)$. It is also noticed that in the above two Figures 2 and 3, there are many small peaks coexisted with the large obvious peaks. The reason for their occurrence is possibly due to the hydrogen migration in the present investigated reactions with light–heavy–heavy mass combination.

From the calculated $PDDCS_{00}$ in Figure 4a, it can be seen that at the same collision energy, the backward scattering of the products is reduced by the isotope substitution, together with the peak position of the backward scattering moving toward smaller scattering angle. But the tendency showing reduced backward scattering with increasing collision energy is quite similar in both reactions. As for $PDDCS_{20}$, it is well known that there exists a limiting value of −0.5 corresponding to that of the alignment parameters $(\theta_r, \phi_r) = (90°, 0°)$ and $(\theta_r, \phi_r) = (90°, 90°)$. Hence, the more the value of $PDDCS_{20}$ approaches to this limiting value, the more the product aligns along the direction perpendicular to $\boldsymbol{k}$. Based on this and seen from Figure 4b, the values of $PDDCS_{20}$ are more negative in D + FCl than in H + FCl and those values near the scattering

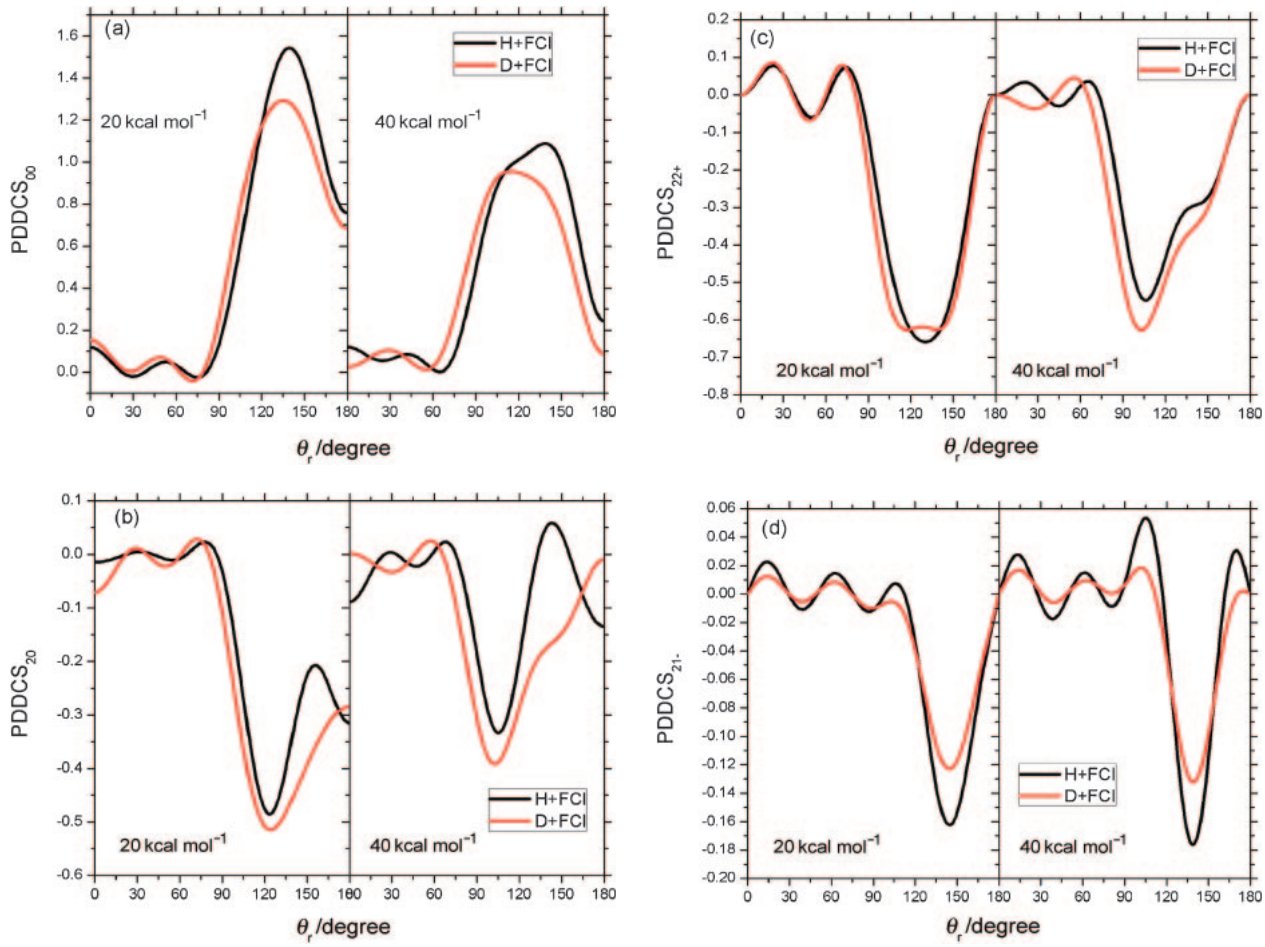


**Figure 4.** Comparison of the PDDCSs distributions between the H + FCl ($v = 0, j = 0$) → HCl + F and the D + FCl ($v = 0$, $j = 0$) → DCl + F reactions for the two collision energies of 20 and 40 kcal mol$^{-1}$. (a) PDDCS$_{00}$, (b) PDDCS$_{20}$, (c) PDDCS$_{22+}$, and (d) PDDCS$_{21-}$.

angle of 120° approach −0.5. Therefore, as indicated by PDDCS$_{20}$, the isotope variant exhibits more product alignment perpendicular to $\boldsymbol{k}$. This is consistent with the above findings from the $P(\theta_r)$ and $P(\phi_r)$ distributions. According to the limiting value of −0.612 of the PDDCS$_{22+}$ corresponding to the limiting value of the alignment parameters $(\theta_r, \phi_r) = (45°, 90°)$, the PDDCS$_{22+}$ in Figure 4c also revealed that the isotope variant has stronger product alignment along the direction of the $\boldsymbol{z} + \boldsymbol{y}$ vector or along the bisection of the $yz$ plane. In addition, isotope substitution influences anisotropy with the scattering angle of the PDDCS$_{21-}$ distribution (Figure 4d) by reducing the extent of the oscillations over the whole angle range, resulting in the less negative values of PDDCS$_{21-}$ in D + FCl than H + FCl. This is in contrast to PDDCS$_{20}$ where the former shows more negative values than the latter. From eq 3, it can be seen that PDDCS$_{20}$ has only a relationship with the $\theta_r$ angle while PDDCS$_{21-}$ has a relationship with both the $\theta_r$ and the $\Phi_r$ angles. Obviously, the isotope effect shown in PDDCS$_{20}$ is expectable from the $P(\theta_r)$ distributions for the two reactions revealing stronger product alignment for the heavier isotope variant, while the isotope effect in PDDCS$_{2-1}$ is a joint consequence of the two different $\theta_r$ and $\Phi_r$ angles obtained for the two reactive systems.

In order to get a more general view of the isotope effect, we further examine the influence of isotope substitution on the $P(\theta_r)$ distribution at 20 kcal mol$^{-1}$ but with the reagent FCl molecule being initially excited to its rotational level $j = 1$–3 or to its vibrational level $v = 1$–3, respectively. Comparison of these $P(\theta_r)$ distributions for the two reactions still revealed that product alignment indicated by $P(\theta_r)$ is stronger in D + FCl than in H + FCl. But the isotope effect does not change the insensitivity to initial rotational excitation of this kind of product alignment. Furthermore, it is found that compared with H + FCl where there is a slightly increasing trend with vibration excitation, the $P(\theta_r)$ distribution in D + FCl becomes rather insensitive to this initial vibration excitation. Figure of this comparison dose not shown to save the space.

Here a question is therefore raised: why can isotope substitution enhance the product polarization in this reaction type of light–heavy–heavy mass combination? We try to explain this with the impulse model that was previously proposed for an A + BC collision system.[34] In this model, the product angular momentum vector $\boldsymbol{j}'$ of HCl can be written as the sum of the following three terms: $j' = L\sin^2\beta + j\cos^2\beta + J_1 m_{Cl}/m_{HCl}$. Here, $\boldsymbol{L}$ and $\boldsymbol{j}$ represent the reagent orbital angular momentum and the reagent angular momentum,

respectively. $J_1 = \sqrt{\mu_{FCl}E_r}(r_{HCl} \times r_{FCl})$, $E_r$ is the repulsive energy, $r_{AB}$ denotes the unit vector where B point to A, and $\mu_{FCl}$ the reduced mass. Previous studies[9,10] have demonstrated that the product polarization is very sensitive to the mass factor $\cos^2\beta = m_H m_F/(m_H + m_{Cl})(m_{Cl} + m_F)$. And there are basically two consequences from an increase in mass factor: less anisotropic distribution or less isotropic distribution of product angular momentum vector $\boldsymbol{j}'$, depending on the type of mass combination or/and on the position of isotope substitution. For example, in studying the light–light–light mass combination reactions of H + HH(D,T), Chen et al.[9] found that an increase of mass factor reduces the anisotropic distributions of $\boldsymbol{j}'$ in H + HH(DT) → HH + H(D,T) while it enhances the anisotropic distributions of $\boldsymbol{j}'$ in H + H(D,T)H → HH(D,T) + H. In the present calculation, the mass factor for the H + FCl and D + FCl reactions is 0.0096 and 0.0188, respectively. Under such conditions, the calculated CM frame product rotational alignment parameter $\langle P_2(\vec{j}' \cdot \vec{k})\rangle$ at collision energy of 20 kcal mol$^{-1}$ is −0.303 and −0.397 for H + FCl and D + FCl, respectively. Therefore, for the present reaction with light–heavy–heavy mass combination, consequences from an increase in mass factor due to isotope effects belongs to the latter case where the isotropic distribution of $\boldsymbol{j}'$ was reduced to a less degree, leading to the more product polarized behaviors in the isotope variant.

## Summary

By applying the quasiclassical trajectory method, we carried out the first dynamic investigation of the H(D) + FCl reactions, with emphasis on examining influences of the isotope substitution on chemical stereodynamics. In the QCT calculation, a batches of 50000 trajectories were running on the DHTSN potential energy surface of the ground electronic state of $1^2A'$ for two collision energies of 20 and 40 kcal mol$^{-1}$, with the initial reagent rovibrational state being set to $v = 0$ and $j = 0$. Further calculations were also carried out for initial rovibrational states $j$ = 1–3 and $v$ = 1–3 at the collision energy of 20 kcal mol$^{-1}$. Comparison between the two reactive systems of all the produced stereodynamic data, i.e., the $P(\theta_r)$, $P(\phi_r)$, and the PDDCSs, has clearly revealed that the products in the isotope variant have stronger polarization behaviors, such as stronger product alignment perpendicular to $\boldsymbol{k}$, stronger product alignment along the direction of $y$ axis, stronger product orientation pointing to the negative direction of $y$ axis, stronger product alignment along the bisection of the $yz$ plane. Mass factor, defined in a previously proposed impulse model for triatomic systems, is very likely responsible for the observed phenomena. In other words, large mass factor in the isotope variant leads to the stronger product polarization for the title reactions with light–heavy–heavy mass combination.

We would like to thank Professor Keli Han for providing us the benchmark stereodynamics code to do the present calculation.

## References

1 D. Sokolovski, J. N. L. Connor, G. C. Schatz, *J. Chem. Phys.* **1995**, *103*, 5979.
2 G. C. Schatz, *Science* **2000**, *288*, 1599.
3 V. Aquilanti, S. Cavalli, D. De Fazio, A. Simoni, T. V. Tscherbul, *J. Chem. Phys.* **2005**, *123*, 054314.
4 T. Yonehara, S. Takahashi, K. Takatsuka, *J. Chem. Phys.* **2009**, *130*, 214113.
5 T.-S. Chu, K.-L. Han, *Phys. Chem. Chem. Phys.* **2008**, *10*, 2431.
6 W. H. Miller, *J. Phys. Chem. A* **2009**, *113*, 1405.
7 T.-S. Chu, Y. Zhang, K.-L. Han, *Int. Rev. Phys. Chem.* **2006**, *25*, 201.
8 M. H. Alexander, D. E. Manolopoulos, H.-J. Werner, *J. Chem. Phys.* **2000**, *113*, 11084.
9 M.-D. Chen, K.-L. Han, N.-Q. Lou, *Chem. Phys. Lett.* **2002**, *357*, 483.
10 M.-L. Wang, K.-L. Han, G.-Z. He, *J. Phys. Chem. A* **1998**, *102*, 10204.
11 R. Sayós, J. Hernando, J. Hijazo, M. González, *Phys. Chem. Chem. Phys.* **1999**, *1*, 947.
12 A. M. G. Ding, L. J. Kirsch, D. S. Perry, J. C. Polanyi, J. L. Schreiber, *Faraday Discuss. Chem. Soc.* **1973**, *55*, 252.
13 E. Würzberg, P. L. Houston, *J. Chem. Phys.* **1980**, *72*, 5915.
14 C. M. Moore, I. W. M. Smith, D. W. A. Stewart, *Int. J. Chem. Kinet.* **1994**, *26*, 813.
15 A. M. Zolot, D. J. Nesbitt, *J. Chem. Phys.* **2007**, *127*, 114319.
16 H. Kornweitz, A. Persky, *J. Phys. Chem. A* **2004**, *108*, 140.
17 A. V. Fishchuk, P. E. S. Wormer, A. der Avoird, *J. Phys. Chem. A* **2006**, *110*, 5273.
18 M. P. Deskevich, M. Y. Hayes, K. Takahashi, R. T. Skodje, D. J. Nesbitt, *J. Chem. Phys.* **2006**, *124*, 224303.
19 B.-Y. Tang, B.-H. Yang, K.-L. Han, R.-Q. Zhang, J. Z. H. Zhang, *J. Chem. Phys.* **2000**, *113*, 10105.
20 M. Y. Hayes, M. P. Deskevich, D. J. Nesbitt, K. Takahashi, R. T. Skodje, *J. Phys. Chem. A* **2006**, *110*, 436.
21 Z.-G. Sun, S. Y. Lee, D.-H. Zhang, *Chin. J. Chem. Phys.* **2007**, *20*, 365.
22 G. Quéméner, N. Balakrishnan, *J. Chem. Phys.* **2008**, *128*, 224304.
23 K.-L. Han, G.-Z. He, N.-Q. Lou, *J. Chem. Phys.* **1996**, *105*, 8699.
24 M.-L. Wang, K.-L. Han, G.-Z. He, *J. Chem. Phys.* **1998**, *109*, 5446.
25 K. L. Han, G. Z. He, N. Q. Lou, *Chin. Chem. Lett.* **1993**, *4*, 517.
26 X. Zhang, K.-L. Han, *Int. J. Quantum Chem.* **2006**, *106*, 1815.
27 F. J. Aoiz, V. J. Herrero, M. P. de Miranda, V. Sáez Rábanos, *Phys. Chem. Chem. Phys.* **2007**, *9*, 5367.
28 F. J. Aoiz, V. J. Herrero, V. S. Rabanos, J. E. Verdasco, *Phys. Chem. Chem. Phys.* **2004**, *6*, 4407.
29 V. Aquilanti, M. Bartolomei, F. Pirani, D. Cappelletti, F. Vecchiocattivi, Y. Shimizu, T. Kasai, *Phys. Chem. Chem. Phys.* **2005**, *7*, 291.
30 V. Aquilanti, F. Pirani, D. Cappelletti, F. Vecchiocattivi, T. Kasai, *Theory of Chemical Reaction Dynamics*, Springer, Netherland, **2004**, Vol. 145, pp. 243–251.
31 G. G. Balint-Kurti, O. S. Vasyutinskii, *J. Phys. Chem. A* **2009**, *113*, 14281.
32 V. Piermarini, A. Laganà, G. G. Balint-Kurti, *Phys. Chem. Chem. Phys.* **2001**, *3*, 4515.
33 T. H. Dunning, *J. Chem. Phys.* **1989**, *90*, 1007.
34 R.-J. Li, K.-L. Han, F.-E. Li, R.-C. Lu, G.-Z. He, N.-Q. Lou, *Chem. Phys. Lett.* **1994**, *220*, 281.